Synthesis, Characterization, and Properties of Covalently Bound, Self-Assembled Porphyrin Multilayer Thin Films

DeQuan Li,* C. Thomas Buscher, and Basil I. Swanson

Isotope and Nuclear Chemistry Division, Los Alamos National Laboratory, University of California, Los Alamos, New Mexico 87545

Received January 14, 1994. Revised Manuscript Received March 18, 1994®

The synthesis and characterization of covalently bound, self-assembled, multilayer thin films of 5,10,15,20-tetra-4-pyridyl-21*H*,23*H*-porphine (TPyP) on fused quartz substrates and the native oxide of silicon ⟨100⟩ surfaces are described. The surface-bound multilayer thin films were grown by anchoring TPyP to a [*p*-(chloromethyl)phenyl]trichlorosilane coupling layer (Cp) and then assembling the sequential TPyP layers via its pyridyl "tether" groups with α,α'-dichloro-*p*-xylene linkers (Ln) to form an alternating layered structure Cp(TPyPLn)$_n$. These self-assembled thin films consist of conjugated porphyrin macrocycle disklike structures that were analyzed by UV–visible spectroscopy, X-ray photoelectron spectroscopy, secondary ion mass spectrometry, and polarized variable-angle, internal attenuated total reflection infrared (PVAI-ATR-IR) measurements. Surface acoustic wave (SAW) mass transduction and electronic absorption spectra reveal that the surface coverage of each layer is a densely packed monolayer (Cp 6.3×10^{-7} mmol/cm^2; TPyP 2.0×10^{-7} mmol/cm^2). Both the film thickness (t = 18 Å for each bilayer) and the average molecular orientation angle (ψ = 43°) of the surface bound chromophores were measured by the PVAI-ATR-IR technique, which are in excellent agreement with polarized, variable-angle second harmonic generation measurements.

Introduction

The sequential deposition of layered materials with desired physical properties offers a promising route to fabricating highly ordered multifunctional thin films.[1] Chemical vapor deposition (CVD) represents a convenient method for fabricating thick films with interesting physical properties. One disadvantage with CVD is a lack of molecular-level control over covalent bonding within the films, as well as to the substrate. Another disadvantage of CVD is that it is very difficult to incorporate functional organic molecules into the deposited thin films because high-temperature evaporation causes decomposition of organic species. The traditional, well-known Langmuir–Blodgett (LB) procedure, in which monolayers at an air-water interface are mechanically transferred to a solid substrate, overcomes several shortcomings of the CVD method. First, the technique is carried out at room temperature, which stabilizes a large number of organic compounds. Second, the LB technique aligns the organic molecules through interactions with the solid substrate. These interactions allow the manipulation of layered films at the molecular-level for constructing nanomaterials. However, conventional LB films are not stable, especially at elevated temperatures,[2] due to the weak van der Waals interactions or hydrogen bonding between interfaces.

Molecular self-assembly strategy,[3] in which mechanical manipulations and complicated ultrahigh-vacuum systems are avoided, is an attractive alternative approach for sequential deposition of layered structures. This method results in improved film adhesion properties by replacing the weak van der Waals forces with covalent bonds, generating much more robust thin films. The self-assembly methodology employs a selective two-dimensional chemistry to directly bond solutes from a homogeneous solution to surface activated sites (e.g., silanols on SiO_2) to form a monolayer spontaneously.[4] The uniformity, film thickness, and surface coverage can be controlled by choosing the appropriate reagent as well as the surface activated sites. Moreover, self-assembly allows stepwise growth, in which the two-dimensional chemistry is designed so that only a molecular monolayer is attached to the surface activated sites during each reaction step. Subsequent layers are linked to the newly formed monolayer surface by activating a different functionality on the previous layer with another chemical treatment. Additional multilayer structures can be built by alternating this pattern repeatedly.

Current studies of these complex (super)molecular self-assemblies, which can be built from either inorganic complexes or organic materials, have been partially motivated by their relevance to a number of potential

* Abstract published in *Advance ACS Abstracts,* April 15, 1994.

(1) (a) Ulman, A. *An Introduction to Ultrathin Organic Films: from Langmuir-Blodgett to Self-Assembly*; Academic Press: Boston, 1991. (b) Chupa, J. A.; Xu, S.; Fishetti, R. F.; Strongin, R. M.; McCauley, J. P., Jr.; Smith, A. B., III; Blasie, J. K. *J. Am. Chem. Soc.* **1993**, *115*, 4383–4. (c) Chen, K.; Caldwell, W. B.; Mirkin, C. A. *J. Am. Chem. Soc.* **1993**, *135*, 1193–4. (d) Li, D.; Smith, D. C.; Swanson, B. I.; Farr, J. D.; Paffett, M. T.; Hawley, M. E. *Chem. Mater.* **1992**, 1047–53. (e) Katz, H. E.; Scheller, G.; Putvinski, T. M.; Schilling, M. L.; Wilson, W. L.; Chidsey, C. E. *Science* **1991**, *254*, 1485. (f) Allara, D. L.; Atre, S. V.; Elliger, C. A.; Snyder, R. G. *J. Am. Chem. Soc.* **1991**, *113*, 1852–1854.

(2) (a) Schildkraut, J. S.; Penner, T. L.; Willand, C. S.; Ulman, A. *Opt. Lett.* **1988**, *13*, 134–6. (b) Lupo, D.; Prass, W.; Schunemann, U.; Laschewsky, A.; Ringsdorf, H.; Ledoux, I. *J. Opt. Soc. Am. B* **1988**, *5*, 300–8. (c) Ledoux, I.; Josse, D.; Vidakovic, P.; Zyss, J.; Hann, R. A.; Gordon, P. F.; Bothwell, B. D.; Gupta, S. K.; Allen, S.; Robin, P.; Chastaing, E.; Dubois, J. C. *Europhys. Lett.* **1987**, *3*, 803–9. (d) Hayden, L. M.; Kowel, S. T.; Srinivasan, M. P. *Opt. Commun.* **1987**, *61*, 351–6.

(3) (a) Kakkar, A. K.; Yitzchaik, S.; Roscoe, S. B.; Kubota, F.; Allan, D. S.; Marks, T. J.; Lin, W.; Wong, G. K. *Langmuir* **1993**, *9*, 388–390. (b) Wilner, I.; Katz, E.; Piklin, A.; Kasher, R. *J. Am. Chem. Soc.* **1992**, *114*, 10965–6. (c) Chailapakul, O.; Crooks, R. M. *Langmuir* **1993**, *9*, 884–8.

(4) (a) Li, D.; Swanson, B. I.; Robinson, J. M.; Hoffbauer, M. A. *J. Am. Chem. Soc.* **1993**, *115*, 6975–6980. (b) Li, D. *Synthesis and Characterization of Chromophoric Self-Assembled Multilayers: Organic Superlattice Approaches to Thin Film Nonlinear Optical Materials*; Ph.D. Thesis, Northwestern University, 1990.

0897-4756/94/2806-0803$04.50/0

technological applications and novel solid-state physical phenomena such as nonlinear optics,[5] monolayer catalysis, smart skins, and chemical microsensors.[6] Many simple self-assembled systems studied in the literature do not have functional properties; as a result they are scientifically interesting but have little practical use. The great challenge in molecular architecture is to incorporate built-in multifunctionalities such as (non)linear optical properties,[5] molecular recognition,[6] or enzyme-mimic catalytic properties into these complex, multimolecular superstructures. In addition to providing structural regularities as well as uniformity and stability, these covalently bound, self-assembly techniques manipulate the molecular module at nanogeometry, as in the case of LB techniques, to ensure proper film thickness and molecular orientation without sophisticated mechanical handling. Furthermore, this methodology may overcome practical problems of conventional LB thin films and other polymeric materials that include long-term stability, poor adhesion to substrates, and polymer swelling. In this work, we demonstrated that covalently bound self-assembled thin films could be exposed to vigorous sonications for a long period of time in various organic solvents without noticeable loss of surface coverage; whereas thin films generated using noncovalent bonding techniques could be easily rinsed off with organic solvents or can be damaged by sonication. We report here the synthesis, characterization, and properties of molecular self-assemblies consisting of a disklike macrocycle complex based on the covalent bonding of 5,10,15,20-tetra-4-pyridyl-21*H*,23*H*-porphine (TPyP) multilayers to a silicon oxide surface. The present molecular building block, TPyP, offers multipyridyl "tether points" which can be built into structurally interlocked networks, with highly delocalized π-electrons on the porphyrin skeleton yielding desired (non)linear optical properties. The growth of the covalently bound, porphyrin based, multilayer molecular self-assembled thin films can be easily monitored using its linear optical property—the distinctive absorption of the porphyrin Soret band.

Experimental Section

All synthetic procedures described below were carried out under an inert, argon atmosphere by employing Schlenk techniques in a well-ventilated fume hood. Chemicals and solvents used in this study were purchased from Aldrich Chemical Co. All solvents were dried and then distilled before use, unless otherwise noted.

1. Substrate Cleaning. Fused quartz plates were purchased from General Electrics and Silicon (Si) wafers were obtained from Siltec Corp. Typical thicknesses for the quartz and the p-doped Si wafers were 1 and 0.5 mm, respectively. Both the 15 cm by 15 cm fused quartz plates and 10-cm-diameter Si wafer disks were cut into approximately 1 cm by 3 cm pieces before use.

The fused quartz substrates were ultrasonically cleaned in a 10% (v/v) Liqui-Nox detergent (Alconox Inc.) solution for 10 min and then refluxed in 1% (w/w) tetrasodium ethylenediamine tetraacetate (EDTA) solution for 10 min, followed by another 10-min sonication in EDTA at ambient temperature. Finally, the substrates were thoroughly rinsed with deionized water and acetone and then sputter cleaned using an argon plasma at a few milliTorr for more than 30 min. Polished p-doped Si wafers were cleaned by sonicating in 10% (v/v) detergent solution for 10 min and then sputter cleaned using an argon plasma for 30 min. All substrates were used immediately after cleaning.

2. Coupling Layer (Cp) Formation. The clean substrates were immersed in a dry $CHCl_3$ solution containing 0.13 M [*p*-(chloromethyl)phenyl]trichlorosilane at room temperature for 24 h. The substrates were transferred into neat $CHCl_3$ and cleaned four times using 2-min sonications. The silane-coated substrates were rinsed using acetone and then dried in air.

3. Porphyrin Layer (TPyP) Addition. A monolayer of the TPyP was covalently attached to the coupling layer by refluxing the Cp-coated substrates with 1.5 mM TPyP in ethanol: chloroform (1:9 by volume) for 2 days at 90–100 °C. The porphyrin-coated substrates were transferred into a mixed solvent of EtOH:$CHCl_3$ (1:9 by volume) followed by a 2-min sonication. This cleaning procedure was repeated three times. After cleaning, the substrates were thoroughly rinsed with acetone and then dried in air.

4. Linker Layer (Ln) Introduction (CpTPyPLn). The CpTPyP monolayer-coated substrates were refluxed in 0.1 M α,α'-dichloro-*p*-xylene in an EtOH:$CHCl_3$ (1:9 by volume) solvent for 2 days at 90–100 °C. The substrates were withdrawn from the solution and sonicated four times in EtOH:$CHCl_3$ (1:9 by volume) with a 2-min duration for each sonication. The self-assembled thin films, terminated with linking functionalities, were rinsed with acetone and then dried in air.

5. Porphyrin Multilayers (Cp[TPyPLn]$_{10}$). The covalently bound, self-assembled porphyrin multilayers were synthesized by alternating steps **3** and **4** until the desired film thickness was obtained. For example, a 10 alternating bilayer of TPyP and Ln was synthesized in this study.

6. Doping of Porphyrin Layer (TPyPBr$_x$). The CpTPyP-derivatized monolayer was immersed in a mixed solvent solution of EtOH:$CHCl_3$ (1:9 by volume) containing 0.97 M bromine at room temperature for 12 h. The substrates were then cleaned by repeated rinsing and sonication in the mixed EtOH:$CHCl_3$ solvent.

PVAI-ATR-IR Measurements. The infrared spectra of porphyrin monolayer and multilayer thin films were collected using a Bio-Rad FTS-40 FTIR with a Harrick Seagull variable-angle internal reflection attachment. The porphyrin monolayer or multilayer was studied using the polarized internal attenuated total reflection (ATR) mode—a technique which allows the angle of incidence to be varied from 5° to 85°. In this mode, the Si wafer functionalized with a porphyrin monolayer or multilayer was pressed against a hemisphere crystal of either ZnSe or Ge with a miniature pressure device to ensure optical contact. Repeatedly pressing the coated Si wafer to either the ZnSe or the Ge hemisphere crystal resulted in identical infrared spectra for both p- and s-polarized geometry; therefore, the monolayer was apparently not damaged or aligned by pressing it against the crystals. A single attenuated total reflection from the interface of the hemisphere crystals and the Si wafers was collected with 1024 scans at 8-cm^{-1} resolution.

Surface Acoustic Wave Mass Transduction. Surface acoustic wave (SAW) resonators (200 MHz) were obtained from Chemical Microsensor Inc., and their resonating frequency was monitored by a Hewlett Packard 5350B microwave frequency counter. When the SAW resonators were removed, rinsed with high-purity organic solvents, and returned back to SAW electronics, the resonating frequency of these SAW resonators remains essentially unchanged (less than 1 kHz). When the SAW resonators were coated with a densely packed monolayer, the resonating frequency shifts more than 8 kHz. Therefore, the mass loading on the surfaces can be measured to assist monitoring the growth of self-assembled thin films.

Results and Discussion

Preparation of Covalently Bound, Self-Assembled Porphyrin Monolayers and Multilayers. The general

(5) (a) Li, D.; Ratner, M. A.; Marks, T. J.; Zhang, C.; Yang, J.; Wang, G. K. *J. Am. Chem. Soc.* **1990**, *112*, 7389–90. (b) Li, D.; Marks, T. J.; Zhang, C.; Yang, J.; Wang, G. K. *SPIE* **1990**, *1337*, 341–7. (c) Li, D.; Marks, T. J.; Zhang, C.; Wang, G. K. *Synthetic Metals* **1991**, *41–43*, 3157–62. (d) Li, D.; Swanson, B. I.; Robinson, J. M.; Hoffbauer, M. A. *SPIE Proc., Nonlinear Opt. III* **1992**, *1626*, 426–30.

(6) (a) Li, D.; Swanson, B. I. *Langmuir* **1993**, *9*, 3341–44. (b) Rubinstein, I.; Steinberg, S.; Tor, Y.; Shanzer, A.; Sagiv, J. *Nature* **1988**, *332*, 426–429. Rubinstein, I.; Rishpon, J.; Sabatani, E.; Redondo, A.; Gottesfeld, S. *J. Am. Chem. Soc.* **1990**, *112*, 6135–6136. (c) Steinberg, S.; Rubinstein, I. *Langmuir* **1992**, *8*, 1183–1187.

Scheme 1

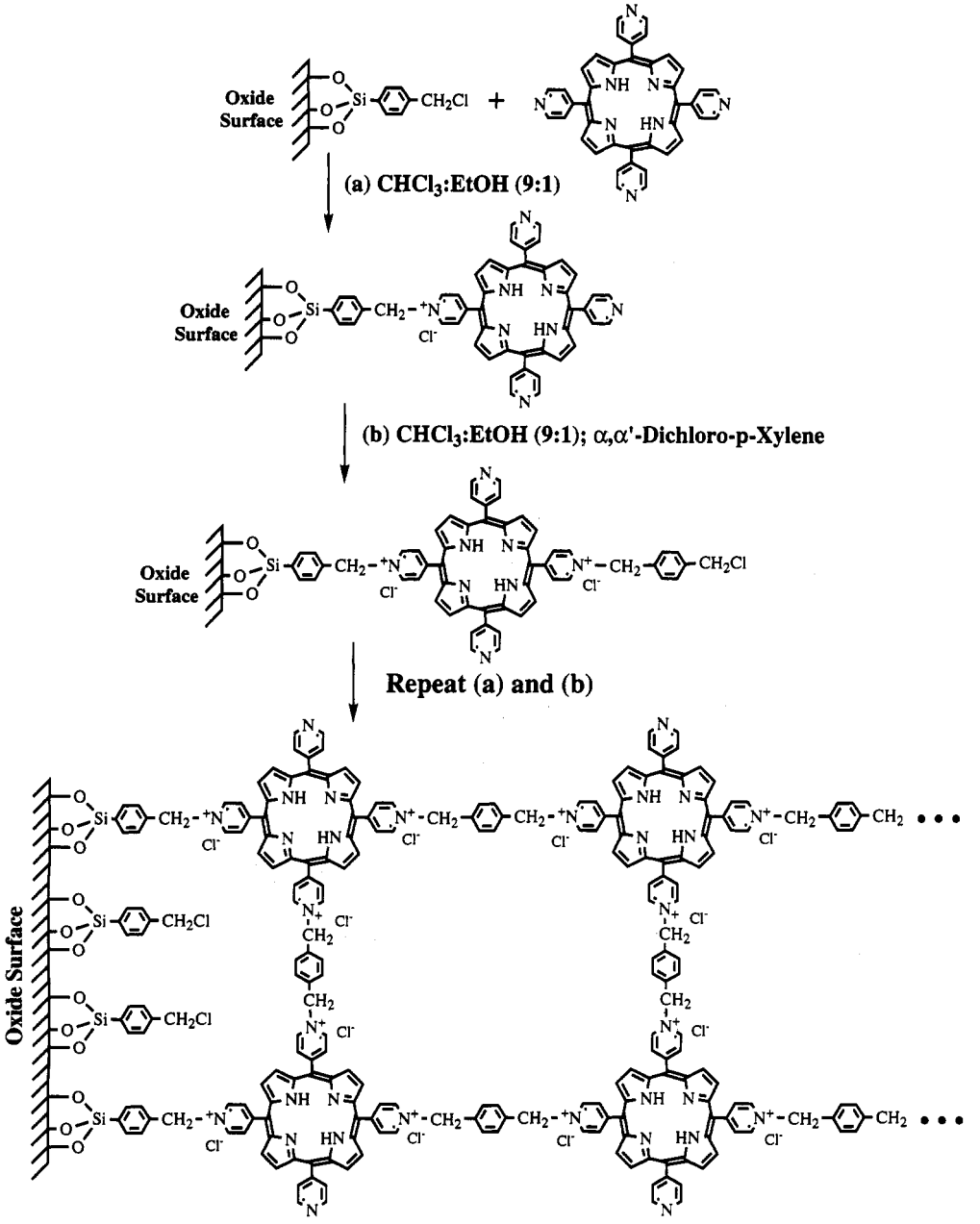

strategy we employed for synthesizing the self-assembled multilayers is summarized with two extreme idealized structures shown in Schemes 1 and 2.[4-6] Various inorganic substrates (Si and quartz wafers) were first functionalized with a [*p*-(chloromethyl)phenyl]trichlorosilane coupling layer (Cp),[7] followed by the anchoring of a 5,10,15,20-tetra-4-pyridyl-21*H*,23*H*-porphine macrocycle onto the substrate to form the self-assembled CpTPyP monolayer (Schemes 1 and 2). A characteristic shift of the optical absorption λ_{max} from 417 to 440 nm in its electronic absorption spectrum,[8] along with its signature (observation of more than one type of nitrogen signals) in X-ray photoelectron spectroscopy (XPS)[9] and surface infrared spectroscopy (vide infra), suggests quaternization of the pyridyl group. The attenuation of the substrate signals (Si and O) in XPS spectra and the absorbance increase in the UV–vis as well as the infrared spectra by the porphyrin monolayer thin films corresponds to a single molecular layer on the fused silica and Si wafer substrates. In the monolayer CpTPyP thin films, the simultaneous appearance of the vibration bands of both pyridyl groups and pyridinium groups in the infrared spectra confirms the quaternization of some pyridyl groups on the porphyrin, that is, an acentric porphyrin structure with pyridinium linkage to the substrate and free pryidyl groups on the outer surface. This acentric structure was also proved by polarized, variable-angle second harmonic generation (SHG) measurements.[4a] The outer pyridyl groups in the CpTPyP film were subsequently linked quaternarily by α,α'-dichloro-*p*-xylene (Ln), followed by additional TPyP for stepwise multilayer growth. Schemes 1 and 2 illustrate two extreme idealized networks of the structurally interlocked aromatic porphyrin TPyP rings linked by α,α'-

(7) Cp layer: $Cl_3SiC_6H_4CH_2Cl + SiO_2$. Advancing contact angle, quartz: $\theta_a(H_2O) = 5°$; Cp: $\theta_a(H_2O) = 50°$. UV–vis: $\lambda_{max} = 195$ nm.

(8) Porphyrin Soret band: $\lambda_{max} \approx 440$ nm (porphyrin-based monolayer, CpTPyP) vs 417 nm for 5,10,15,20-tetra-4-pyridyl-21*H*,23*H*-porphine in chloroform.

(9) XPS: C(1s), N(1s), O(1s), Si(2s and 2p), and Cl(2p) or I(3d).

Scheme 2

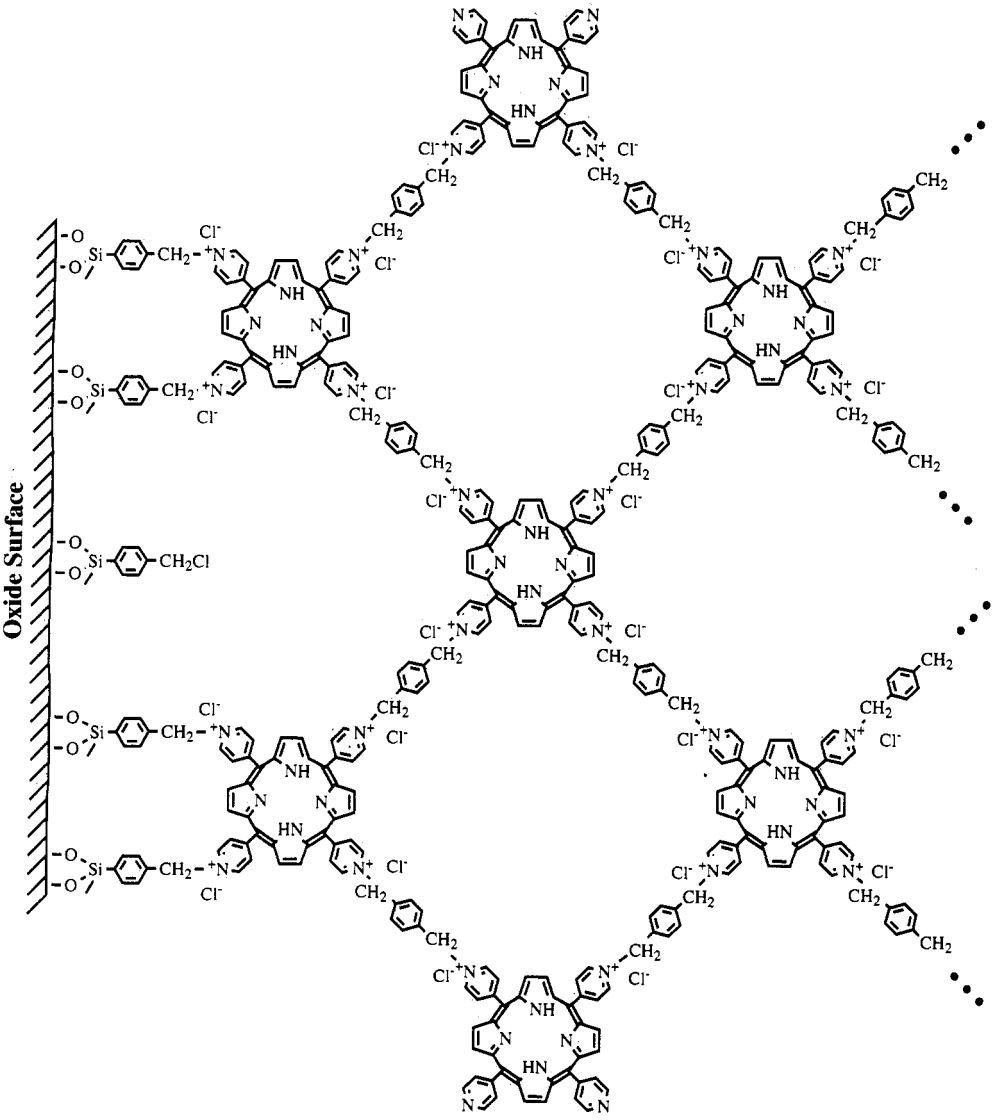

dichloro-*p*-xylene via covalent bonds. This alternating TPyP and Ln bilayer structure was indicated by the almost complete disappearance of the pyridyl group vibration mode and the corresponding increase in intensity of the pyridinium group vibrational mode in the infrared spectra, which is consistent with a fully quaternized tetra-4-pyridylporphyrin moiety. These multilayer additions of TPyP can be conveniently monitored by the increase of the absorbance of the porphyrin Soret band at $\lambda_{max} \approx 440$ nm. A linear relationship between the absorbance and the number of TPyP layers was obtained as shown in Figure 1. This result is significant because it indicates that the amount of material deposited for each layer is essentially the same, and thus the growth of thicker films is feasible.

Structure and Bonding of Self-Assembled Porphyrin Multilayers. In the area of molecular assemblies, the bonding at interfaces (e.g., between the substrate and a self-assembled monolayer or within multilayers) is usually ambiguous due to the lack of characteristic signatures in available techniques to identify the formation of these bonds. For instance, whether the bonding between alkanethiols and gold is covalent, ionic or coordinative is not clearly understood. Our system Cp[TPyPLn]$_n$, however, has a unique informative pyridinium vibrational mode which can be used to monitor the new layer formation upon quaternization reaction at the pyridyl position. Using PVAI-ATR-IR techniques, we can monitor this pyridinium mode, hence monitor the growth of self-assembled mul-

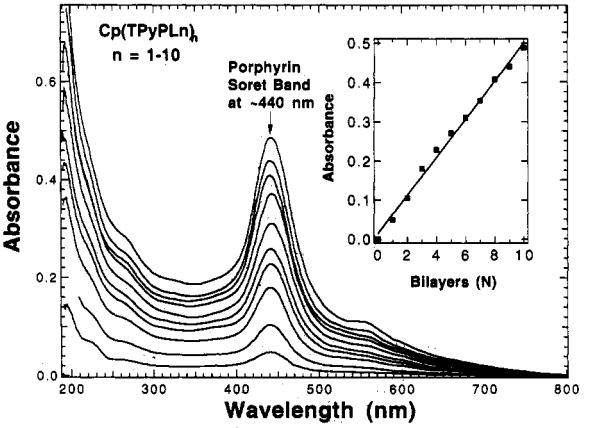

Figure 1. Optical absorption of covalently bound, self-assembled porphyrin multilayers Cp(TPyPLn)$_n$ (n = 1–10) on a quartz substrate. The spectra were collected from two individual multilayer thin films on both sides of the quartz substrate, therefore, each individual monolayer has only half of the intensity shown in the graph. Inset: A linear relationship between the absorbance and the number of bilayers (TPyPLn), N.

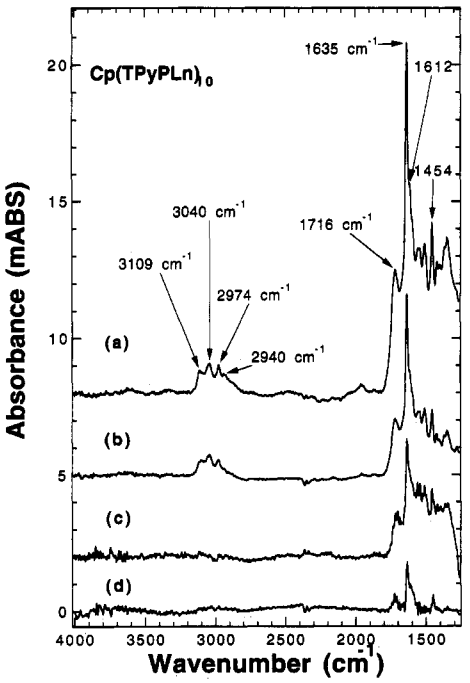

Figure 2. PVAI-ATR-IR spectra of 10 layers of self-assembled porphyrin multilayer thin films, $Cp(TPyPLn)_{10}$, covalently bound to the native oxide of Si⟨100⟩ surfaces. For (a) and (c), p-polarized light at incidence of 39° and 60° was used; and for (b) and (d), s-polarized light at incident angle of 39° and 60° was used. The internal reflection element (IRE) was ZnSe, and 1024 scans at 8-cm^{-1} resolution were collected. The baseline was corrected to zero absorbance and offset for display purposes. Note that Si wafer starts to absorb below 1430 cm^{-1}.

tilayer thin films, and therefore, understand the bonding nature between TPyP and Ln or Cp layers. Although the bonding and molecular structure information can be obtained from spectroscopy techniques, thin-film structure of these self-assemblies still remains poorly understood. The experimental results are that most of the pyridyl groups (a very weak pyridyl shoulder at 1593 cm^{-1}, see Figure 2) are consumed (>95%) during the quaternization reactions but little is known about the lateral cross-linking or the percentage of conversion about the chloromethyl groups by the pyridyl groups. In another study,[4a] the TPyP monolayer was reacted with iodomethane using similar reaction conditions, and the vibration mode (1953 cm^{-1}) of pyridyl groups once again disappeared completely while the pyridinium mode (1635 cm^{-1}) doubled in its intensity. This result, along with approximate equal intensities for both pyridyl and pyridinium modes in the monolayer samples, favors Scheme 2 structure, i.e., the amount of pyridyl groups equals that of pyridinium groups. The real order in these thin films can be best described by the alternating two-dimensional (i.e., in the plane of substrates) glassy state of Ln layers and TPyP layers with a general alignment along surface normal and a tendency toward order. Although little is known about the degree of lateral cross-linking, the covalent bound porphyrin thin films are extremely robust and can tolerate rigorous sonication and washing in various organic solvents.

Surface Coverage. To determine the Cp coverage, the silane based Cp is bound to the surface oxide (SiO_2) of a surface acoustic wave (SAW) resonator via a siloxane linkage.[7] The formation of a self-assembled Cp monolayer on the SAW resonator causes a frequency shift of −8.5 kHz. The total mass loading due to the formation of covalently bound, self-assembled Cp monolayer is given by eq 1, where $K = -1.3 \times 10^{-6}$ s cm^2/g, Δm = mass change,

$$\Delta f = KF^2\Delta m/A \quad (1)$$

A = surface area, F = resonating frequency (200 MHz), and Δf = frequency shift.[10] The surface coverage for the Cp layer was 6.3×10^{-7} mmole/cm^2 or 3.8 molecules/100 Å^2, according to eq 1. The density of surface hydroxyl groups for crystalline silica is approximately 5.0 hydroxyl groups/100 Å^2,[11] and the SAW result suggests that about 80% of the surface hydroxyl groups react with [*p*-(chloromethyl)phenyl]trichlorosilane (Cp). By utilization of the strong porphyrin Soret band at $\lambda_{max} \sim 440$ nm, the TPyP surface coverage, $d_{surf.} = A\epsilon^{-1}$ [mmol/cm^2], can be quantitatively deduced. The extinction coefficient was determined from a model compound, 5,10,15,20-tetrakis-(1-methyl-4-pyridyl)-21*H*,23*H*-porphine tetra-*p*-tosylate salt ($\lambda_{max}(H_2O)$ = 422 nm; $\epsilon = 1.5 \times 10^5$ cm^{-1} M^{-1}). The estimated surface density[12] of the porphyrin macrocycle TPyP is $\sim 2.0 \times 10^{-7}$ mmol/cm^2, or ~1.2 porphyrin macrocycle/100 Å^2. Assuming a 2:1 reaction ratio of Cp molecules to porphyrin, these results reveal that approximately two-thirds of the Cp was used in the quaternization reactions as illustrated in Scheme 2 which was favored by the PVAI-ATR-IR results (vide supra). Alternatively, if one assumes a 1:1 reaction ratio, about one-third of the Cp was converted to the product (Scheme 1). This less than 100% conversion is due to the limited surface-area available on the two-dimensional substrate rather than to the reactivity of a particular functional group. Although the porphyrin surface coverage is about a factor of three smaller than the Cp layer, it is more than four times larger than that of the Cp molecule. Thus, both Cp and TPyP layers are densely packed even though they have different molecular number densities. This difference is accounted for by the individual molecular space filling properties.

Polarized Variable-Angle Internal Attenuated Total Reflection Infrared Spectroscopy (PVAI-ATR-IR). PVAI-ATR-IR spectra of CpTPyP monolayers have been reported previously,[4a] and we will summarize only the major features of these spectra. The PVAI-ATR-IR spectra was obtained with a single reflection from the interface of a ZnSe or Ge and Si/porphyrin monolayer in both p- and s-polarizations at various incident radiation. The spectra showed a pyridyl ν_4 mode at 1593 cm^{-1} and a N-substituted pyridinium ν_{8a} mode at 1635 cm^{-1}, both of which are attributable to quaternization reactions.[13] These two IR bands suggest that the porphyrin thin films are polar, confirmed by the observation of large second harmonic generation (SHG) in these materials. In addition to the above major features, the vibrations at 1716, 1500, and 1450 cm^{-1} were also observed and attributed to the porphyrin skeleton modes.[14]

(10) (a) Grate, J. W.; Klusty, M. *Anal. Chem.* **1991**, *63*, 1719–27. (b) Grate, J. W.; Snow, A.; Ballantine, D. S., Jr.; Wohltjen, H.; Abraham, M. H.; McGill, R. A.; Sasson, P. *Anal. Chem.* **1988**, *60*, 869–75.

(11) Wasserman, S. R.; Whitesides, G. M.; Tidswell, I. M.; Ocko, B. M.; Pershan, P. S.; Axe, J. D. *J. Am. Chem. Soc.* **1989**, *111*, 5852–61.

(12) Porphyrin monolayer absorbance at $\lambda_{max} \approx 440$ nm: $A = 0.0295$; model compound 5,10,15,20-tetrakis(1-methyl-4-pyridyl)-21*H*,23*H*-porphine (tetra-*p*-tosylate salt): $\lambda_{max}(H_2O)$ = 422 nm ($\epsilon = 1.5 \times 10^5$ cm^{-1} M^{-1}).

(13) (a) Bunding, K. A.; Bell, M. I.; Durst, R. A. *Chem. Phys. Lett.* **1982**, *89*, 54–58. (b) Kobayashi, Y.; Itoh, K. *J. Phys. Chem.* **1985**, *89*, 5174–5178. (c) Long, D. A.; George, W. O. *Spectrochim. Acta* **1963**, *19*, 1777–1790. (d) Spinner, E. *Aust. J. Chem.* **1967**, *20*, 1805–13.

Figure 2 shows the PVAI-ATR-IR spectra of 10 layers of covalently bound, self-assembled Cp(TPyPLn)$_{10}$ thin films. In these spectra, the weak C–H vibrations from both aromatic Ar–H at 3109 and 3040 cm^{-1} and aliphatic CH_2 at 2974 and 2940 cm^{-1} were clearly observed for the 10-layer film at 39° incidence with ZnSe as the internal reflection element (IRE). As in the case of the CpTPyP monolayers, the porphyrin skeleton vibrations at 1716, 1500, and 1450 cm^{-1} were clearly resolved. The band at 1716 cm^{-1} is associated with the vibration of C_α–C_m in the porphyrin skeleton, whereas the vibration at 1450 cm^{-1} arises from a combination of $\nu(C_\beta$–N) and δ(CCN)[15] and is attributable to the porphyrin ring (Figure 2). One must be careful at assigning the 1400-cm^{-1} vibration to the phenyl mode of the Cp layers,[16] because the substrate Si wafer starts to absorb below 1430 cm^{-1} and it can be masked by the Si absorptions. The major features in these spectra include the strong pyridinium mode at 1635 cm^{-1} and the absence of the pyridyl mode at 1593 cm^{-1}, which is consistent with a structurally interlocked self-assembled thin films. The critical incident angle, $\theta_c = 39°$, yields the maximum signal because a strong interaction of the infrared radiation with the interface of the ZnSe hemisphere crystal and the Si wafer occurs at this geometry. As the incident angle is tuned to $\theta = 60°$, only the strongest absorptions such as the pyridinium mode at 1635 cm^{-1} and porphyrin frame mode at 1716 and 1450 cm^{-1} were observed. The weak C–H vibrations disappeared in the noise. It is important to note, that although a vibration band is not observed in an IR spectrum, this does not necessarily mean that it is not a symmetry allowed IR vibration or absent alltogether in the thin film. For example, in both p- and s-polarized spectra, the CH_2 and Ar–H bands were not resolved at 60° incidence, but these IR bands were clearly observed at 39° incident angle.

Orientation of Surface-Bound Porphyrin Monolayers in Self-Assembled Thin Films. The molecular orientation information deduced from both SHG measurements and PVAI-ATR-IR spectroscopy for the CpTPyP monolayer has been discussed in depth in our previous studies.[4a] The second order susceptibility tensor ratio $\chi_{zzz}/\chi_{zxx} = 2\cot^2\langle\psi\rangle$ determined from both variable-angle and polarized SHG measurements yields an average molecular orientation of $\langle\psi\rangle = 43 \pm 3°$, which can also be obtained from PVAI-ATR-IR measurements (pyridyl mode: $A_p/A_s = 1.7$, $\langle\theta\rangle = 43°$). This molecular orientation angle, $\langle\theta\rangle$, is in excellent agreement with the polar angle, $\langle\psi\rangle$, measured using polarized surface SHG. The absorbance ratio of the pyridinium mode for a 10-layer thin film in these two polarizations, $A_p/A_s = 1.9$, remains relatively constant, indicating that the molecular alignment has not been altered significantly by the structurally interlocked multilayer growth.

Film Thickness. The PVAI-ATR-IR spectra for the film thickness measurements were carried out with an IRE of Ge ($n_1 = 4.0$) crystal hemisphere at 45° incident angle. The covalently bound, self-assembled thin film ($n_2 = 1.5$) was pressed against the Ge hemisphere crystal with a miniature device to ensure optical contact. The film thickness of porphyrin self-assembled monolayers or multilayers can be calculated by integrating the electric field of the evanescent wave when internal total reflection occurs. The theoretical rationale for this experimental geometry was demonstrated to be valid by others.[17] The absorbance A of a particular IR band in PVAI-ATR-IR spectra was given by Harrick as

$$A = \frac{n_2}{n_1}\frac{\alpha}{\cos\theta}\int_0^t E^2\,dz \qquad (2)$$

where n_1 and n_2 are refractive indexes of the IRE (Ge) and the self-assembled thin film respectively, and α is the absorption coefficient per unit thickness.[18] The evanescent wave E decays exponentially upon penetrating the thin film. Its decay can be expressed by the following equation:[19]

$$E = E_0\exp(-z/d_p) \qquad (3)$$

The depth of penetration d_p, defined as the distance required for the electric field amplitude to fall to e^{-1} of its value at the interface, is given by the equation

$$d_p = \lambda/2\pi[\sin^2\theta - (n_2/n_1)^2]^{1/2} \qquad (4)$$

where E_0 is the amplitude of the evanescent wave at the interface between the IRE (Ge) and the self-assembled thin films, z is the depth from the interface, λ is the wavelength of the infrared radiation, and θ is the incident angle. By integration of eq 2, the absorbance of a particular IR band of the surface-bound self-assembly is obtained and can be expressed by the equation

$$A_t = A_\infty[1 - \exp(-2t/d_p)] \qquad (5)$$

A_∞ is the absorbance of a infinitely thick film, i.e., $E \to 0$ while $t \to \infty$, and can be simulated from a liquid cell which is so thick that the infrared radiation cannot penetrate it and the amplitude of the evanescent wave decays to a negligible level. The pyridyl mode at approximately 1593 cm^{-1} was studied because it is easy to find model compound in liquid state with characteristic pyridyl vibration band, for example, 4-ethylpyridine. In p-polarized geometry, the absorbance A_∞ of a thin film with perfect alignment along the z direction is a factor of 3 larger than that of a solution $A_\infty/3 = A_{soln} = 0.119$. The observed pyridyl mode intensity in the CpTPyP system with self-assembled monolayers on both sides is $2A_t = 6.15 \times 10^{-3}$. The film thickness of a self-assembled porphyrin monolayer as calculated from eq 5 is $t = 18$ Å. Using a molecular thickness of 23.4 Å obtained from averaged crystallographic porphyrin bond lengths and bond angles for the chromophore layer, standard bond distances for the coupling layer, and an average polar angle of $\langle\psi\rangle$ of ~43° (vide supra), a monolayer CpTPyP film

(14) (a) Ogoshi, H.; Saito, Y.; Nakamoto, K. *J. Chem. Phys.* **1972**, *57*, 4194–4202. (b) Sunder, S.; Bernstein, H. J. *J. Raman Spectrosc.* **1976**, *5*, 351–371. (c) Alben, J. O. *The Porphyrins*; Academic Press: New York, 1978; Vol. III, pp 323–345.

(15) C_α, C_β, and C_m stand for α, β, and *meso* carbon atoms.

(16) (a) Mair, R. D.; Hornig, D. F. *J. Chem. Phys.* **1949**, *17*, 1236–47. (b) Thakur, S. N.; Goodman, L.; Ozkabak, A. G. *J. Chem. Phys.* **1986**, *84*, 6642–56. (c) Richardson, N. V. *Surf. Sci.* **1979**, *87*, 662–8. (d) Busca, G.; Zerlia, T.; Lorenzelli, V.; Girelli, A. *J. Catal.* **1984**, *88*, 131–6. (e) Koel, B. E.; Crowell, J. E.; Mate, C. M.; Somorjai, G. A. *J. Phys. Chem.* **1984**, *88*, 1988–96.

(17) Ohta, K.; Iwamoto, R. *Appl. Spectrosc.* **1985**, *39*, 418–425.

(18) Harrick, N. J. *J. Opt. Soc. Am.* **1965**, *55*, 851.

(19) (a) Harrick, N. J. *Internal Reflection Spectroscopy*; John Wiley & Sons: New York, 1967. (b) Harrick, N. J.; Mirabella, F. M. *Internal Reflection Spectroscopy: Review and Supplement*; Harrick Scientific Corp.: New York, 1985.

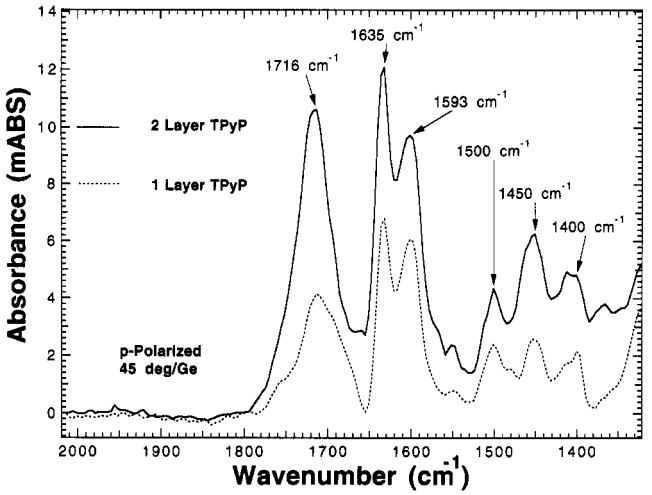

Figure 3. PVAI-ATR-IR spectra of a self-assembled monolayer (CpTPyP, dotted line) and a porphyrin bilayer (CpTPyPLnT-PyP, solid line) thin film covalently bound to the native oxide of a Si⟨100⟩ surface with p-polarized light at an incidence of 45°. The internal reflection element (IRE) was Ge, and 1024 scans at 8-cm^{-1} resolution were collected. The baseline was corrected to zero absorbance and offset for display purposes. Note that Si wafer starts to absorb below 1430 cm^{-1}.

thickness of ~17 Å was calculated.[20,21] The film thickness measured from PVAI-ATR-IR experiments agrees well with the crystallographic estimation. By employing the estimated thickness of ~18 Å and a surface coverage of ~2.0 × 10^{-7} mmol/cm^2, a molecular packing density of 1 porphyrin/1.1 nm^3 was obtained. The crystallography packing density[22] of TPyP is 1 molecule/0.99 nm^3. Thus, the covalently bound, self-assembled porphyrin monolayers are almost as densely packed as a single crystal of TPyP. This result of a densely packed monolayer is also confirmed by the broadening of the porphyrin Soret band in the electronic absorption spectra, which arises from close intermolecular packing and the cofacial intermolecular π-electron interactions in condensed solid-state thin films.

Equation 5 can be also used to monitor thin-film growth. If the film thickness t is very small when compared to the penetration depth d_p, which is on the order of 0.1–1 μm, eq 5 can be simplified to

$$A_t = 2A_\infty t/d_p \qquad (6)$$

Equation 6 suggests that the infrared intensity of a particular band will grow linearly for ultrathin films ($t \leq$ 25 nm). Figure 3 presents the PVAI-ATR-IR spectra of a monolayer CpTPyP and a double layer of CpTPyPLnCpTPyP. The spectra was obtained using a Ge IRE at 45° incident with p-polarized geometry. The absorbance increases for the IR bands at 1716, 1635, 1593, 1500, 1450, and 1400 cm^{-1} are 2.6, 1.8, 1.6, 1.8, 2.4, and 2.1, respectively. These results suggest that the thickness of the second layer is basically the same as that of the first layer or that the bilayer films are approximately twice as thick as monolayer thin films.

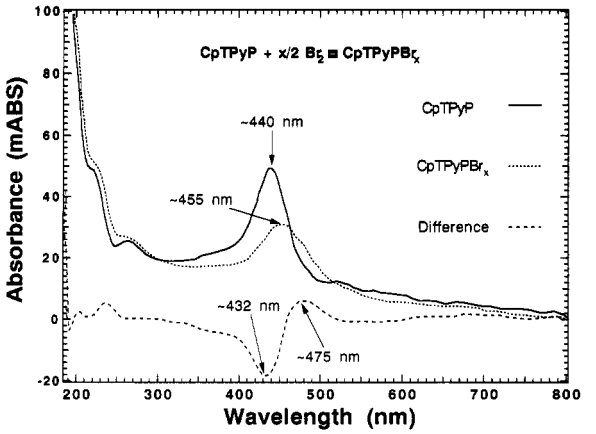

Figure 4. Optical absorption of a covalently bound, self-assembled porphyrin monolayer on a quartz substrate before CpTPyP (solid line) and after CpTPyPBr$_x$ (dotted line) doping with Br$_2$. The spectra are collected from two individual monolayer thin films on both sides of the quartz substrate; therefore, each individual monolayer has only half of the intensity shown in this graph.

In our previous study,[4a] the porphyrin monolayer was quaternized by iodomethane to form CpTMPyP monolayer and the PVAI-ATR-IR spectra were carried out with an IRE of ZnSe (n_1 = 2.4) crystal hemisphere at 39° incident angle. For the pyridinium mode at 1635 cm^{-1}, the experimental absorbance value for a monolayer of CpTMPyP is $A_{1\text{-layer}}$ = 1.26 mABS; whereas the measured absorption for 10 layers of Cp[TPyPLn]$_{10}$ is $A_{10\text{-layer}}$ = 12.9 mABS (Figure 2). This factor of 10 ratio for the pyridinium vibration band was in excellent agreement with the UV–vis results which support the linear relationship between the absorbance and the number of TPyP layers.

Judging from the results of the optical film thickness, t, derived from PVAI-ATR-IR spectra, the accuracy of this technique is about ±20%, because the IR band absorption intensities are usually not very quantitative. This technique, however, is quite informative when used to estimate the order of magnitude of self-assembled thin-film thickness. Thus, we conclude that the intensity of an infrared band for a typical monolayer (~20 Å) is on the order of milliabsorbance units while using PVAI-ATR-IR techniques. This result is well-supported by the data in the literature.[23]

Doped Self-Assembled Thin Films. Self-assembled porphyrin monolayers or multilayers can be doped with Br$_2$ by immersing the substrates coated with CpTPyP thin films in a 0.97 M bromine solution with a 9:1 (v/v) ratio of CH_3Cl and EtOH as the solvent. The presence of Br$^-$ in the covalently bound, self-assembled monolayer film of CpTPyPBr$_x$ is confirmed by the observation of the negative ions ^{79}Br$^-$ and ^{81}Br$^-$ in the static secondary ion mass spectrometry (SIMS) spectra. Careful SIMS experiments will also resolve the chlorine ions ^{35}Cl$^-$ and ^{37}Cl$^-$ in the self-assembled CpTPyPBr$_x$ films. The mass intensities of both halides match their natural abundance. While using the X-ray photoelectron spectroscopy (XPS), the following elements were found; O(1s) at 532.0 eV, Si(2s,-2p) at 153.0 eV and 103.4 eV, Cl(2p) at 199.6 eV, C(1s) at

(20) Smith, K. M. *Comprehensive Heterocyclic Chemistry*; Pergamon Press: New York, 1984; p 386.
(21) Lide, David R. *Handbook of Chemistry and Physics*, 72nd ed.; CRC Press: Boston, 1991; pp 9-2–9-17.
(22) (a) Fleischer, E. B.; Stone, A. L. *Chem. Commun.* **1967**, 332–3. (b) Fleischer, E. B.; Shachter, A. M. *Inorg. Chem.* **1991**, *30*, 3763–9.
(23) (a) Laibinis, P. E.; Whitesides, G. M.; Allara, D. L.; Tao, Y. T.; Parikh, A. N.; Nuzzo, R. G. *J. Am. Chem. Soc.* **1991**, *113*, 7152–7167. (b) Nuzzo, R. G.; Fusco, F. A.; Allara, D. L. *J. Am. Chem. Soc.* **1987**, *109*, 2358–2368. (c) Nuzzo, R. G.; Dubois, L. H.; Allara, D. L. *J. Am. Chem. Soc.* **1990**, *112*, 558–569.

284.5 eV, and N(1s) at 400.0 eV in the undoped surface-bound monolayer thin films, CpTPyP. After doping with Br_2, photoelectrons of Br(3d) at 70.0 eV were clearly observed, which is consistent with the formation of $CpTPyPBr_x$ monolayers. The amount of Br^- estimated from the XPS spectra is $x = 0.78–1.85$.

The doping of the self-assembled porphyrin monolayers is also manifested in the electron absorption spectra. As indicated in Figure 4, the oxidization of CpTPyP monolayers causes the porphyrin Soret band to red-shift about 15 nm from ~440 to ~455 nm with maximum depletion at ~432 nm and strongest increase at ~475 nm. The red-shift of the porphyrin Soret band indicates the oxidation of the porphyrin skeleton upon doping with Br_2, that is, the removal of π-electrons due to bromine oxidization is from the conjugated porphyrin skeleton framework rather than from pyridyl groups, which are typically perpendicular to the porphyrin plane.

In the PVAI-ATR-IR spectra (Figure 5), the doped self-assembled porphyrin films show nearly identical IR vibrations to those of undoped porphyrin films. The only difference is that the pyridyl mode and pyridinium mode broaden slightly and the porphyrin skeleton mode at ~1716 cm^{-1} broadens significantly. These results suggest that the bromine oxidization occurs mainly at the porphyrin skeleton, which is consistent with the red-shift of the porphyrin Soret bands. The broadening of the IR features is consistent with the removal of the valence electrons and the creation of holes or conduction bands in the materials. As materials change from insulator to conductor, the IR vibrations shift from sharp, well-defined bands to featureless spectra. However, it is important to point out that the relative intensities and profiles of these IR bands can also be affected by several other factors such as structural inhomogeneity, penetration depth, and life time of excited vibrational states. The doped self-assembled $CpTPyPBr_x$ film shows no appreciable conductivity due to ultrathin-film structure and lack of continuity in the plane of supports. The incorporation of small bromine ions into the self-assembled thin films has not perturbed the porphyrin orientation significantly as indicated by a constant absorbance ratio of both the pyridyl and the pyridinium IR bands in p- and s-polarized spectra before and after the bromine doping. The pyridyl and pyridinium absorption intensities remain relatively unchanged in the doping reaction, which further suggests that the self-assembled films were very robust and can accommodate bromine incorporation.

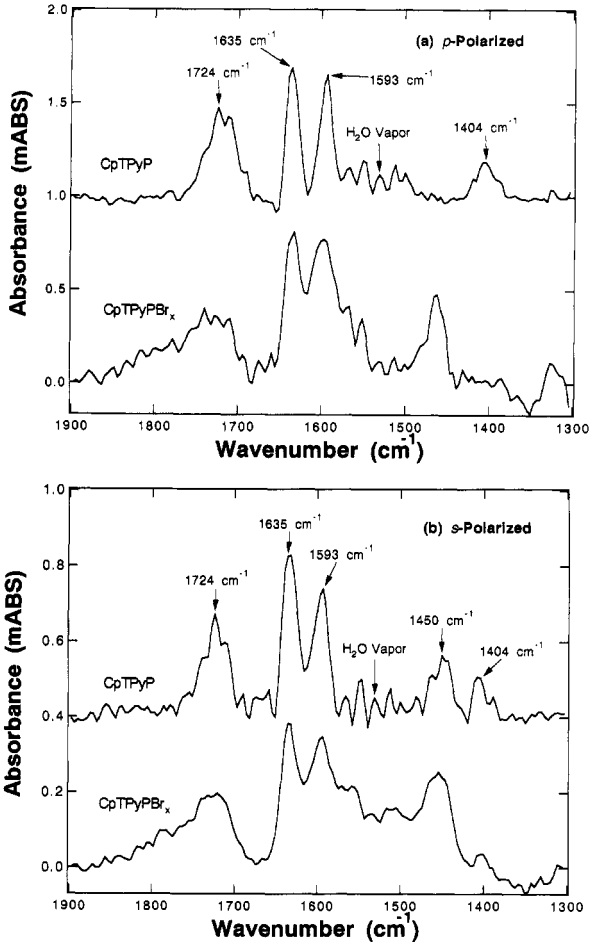

Figure 5. PVAI-ATR-IR spectra of a self-assembled porphyrin monolayer thin films covalently bound to the native oxide of a Si⟨100⟩ surface, before (CpTPyP, top) and after ($CpTPyPBr_x$, bottom) Br_2 was doped. For (*a*), p-polarized light at incidence of 39° was used; and for (*b*), s-polarized light at incident angle of 39° was used. The internal reflection element (IRE) was ZnSe, and 1024 scans at 8 cm^{-1} resolution were collected. The baseline was corrected to zero absorbance and offset for display purposes. Note that Si wafer starts to absorb below 1430 cm^{-1}.

Conclusions

We have studied both the film thickness and molecular orientation using the PVAI-ATR-IR technique for covalently bound, self-assembled monolayer and multilayer porphyrin thin films. The average molecular orientation of the porphyrin monolayer was 43° relative to the surface normal of the substrate, and the monolayer thickness was approximately 18 Å. This technique, along with SAW mass transduction and electronic absorption spectroscopy, reveals that the porphyrin multilayer is highly ordered and closely packed in its solid-state structure. The constant absorbance ratio A_p/A_s in the PVAI-ATR-IR spectra and the linear growth of the porphyrin Soret band in the electronic spectra suggest that the multilayer packing structure and molecular orientation are essentially identical to those of a monolayer. The present CpTPyP thin films are quite robust and can be doped with Br_2 to yield an oxidized porphyrin monolayer of $CpTPyPBr_x$.

Acknowledgment. This work was performed under the auspices of the Department of Energy. The authors acknowledge the support of the Center for Material Science at Los Alamos National Lab, the Division of Materials Science of the DOE Basic Energy Sciences, and the Laboratory Directed Research and Development program. We thank M. T. Paffett and J. D. Farr for performing the SIMS and XPS measurements.